
EXPERIMENTAL RESEARCHES OF THE DECAY COEFFICIENT OF NONIDEAL PLASMA PRODUCED AT PULSED DISCHARGES IN WATER

O.A. FEDOROVICH, L.M. VOITENKO

UDC 533.9.621.039.66
©2008

Institute for Nuclear Research, Nat. Acad. Sci. of Ukraine
(47, Nauky Ave., Kyiv 03680, Ukraine; e-mails: oafedorovich@kinr.kiev.ua, lmvoiten@kinr.kiev.ua)

The decay coefficient of nonideal plasma (NP) produced at pulsed discharges in water (PDW) has been measured experimentally in one of the discharge modes, and the results obtained have been compared with those calculated theoretically. The revealed discrepancy between them was found to be of 5 to 6 orders of magnitude, with lower values corresponding to the experimental procedure. The available theoretical models cannot provide a satisfactory agreement with experiment, so that the further development of the model describing the recombination in NP is needed.

1. Introduction

In recent decades, the interest to researches dealing with NP has been considerably growing. This fact is associated with the implementation of some power-production projects and the development of facilities, where NP is planned to be used as a working body. These include powerful magnetohydrodynamic generators, power installations and rocket engines with gas-phase nuclear reactors, powerful optical and x-ray lasers with nuclear pumping, some devices of plasma-chemical industrial technology, thermonuclear power installations, thermoelectric converters of energy, electrohydropulse installations, devices for switching-off and commutating high-voltage installations and networks, accelerators of the "railotron" type, powerful pulse light sources, *etc.* [1].

Experimental researches of NP properties are also important for the development of fundamental ideas concerning the state of a substance under extreme conditions, which have been studied very poorly. A serious hindrance to the development of NP theory is the absence of reliable experimental data on the interrelation between the parameters of NP and its properties, especially optical ones. Such a situation in experimental domain has become a result of a few reasons associated with difficulties one faces while generating and studying NP with a rather high degree of

nonideality, and the absence of both reliable techniques for measuring the NP parameters and the corresponding equipment. As a rule, under laboratory conditions, NP has very short lifetimes (micro and milliseconds). Moreover, at pulsed electric discharges, high currents of tens and hundreds of kiloamperes run through, and high voltages of tens of kilovolts are applied across a discharge gap, which complicates the measurement procedure.

Experimentally, the recombination processes in a dense NP have been little studied. In order to calculate the NP parameters and construct the corresponding models, it is necessary to know the coefficients of ionization and recombination, the lifetimes of ions and electrons, as well as their dependences on the temperature and the electron concentration. For instance, the coefficients of ionization and recombination in plasma are experimentally determined for electron concentrations N_e which are not higher than $2 \times 10^{17} \text{ cm}^{-3}$ [2, 3].

As the classical theoretical works concerning the calculations of the coefficients of ionization and recombination in plasma, we mention [3–6]. Lately, work [7] was published, where the coefficient of recombination was calculated for the electron concentrations up to 10^{17} cm^{-3} and in a wide temperature range. In those works, however, calculations were carried out for isolated hydrogen atoms, and the effects of nonideality were not taken into account. In work [8], while calculating the coefficient of recombination α , an attempt was made to consider the disappearance of the upper lines in the Balmer series, which brought about a reduction of α in a number of cases. However, the coefficients of electron capture onto actual atomic levels were assumed at that to be approximately equal to those for an isolated atom [8]. Unfortunately, such an assumption is not always applicable to NP, because the atomic levels become strongly broadened in strong plasma microfields, which are comparable with the field of an atom (for instance,

the broadening of the H_α line amounts to ± 30 nm at the electron concentration of about 10^{19} cm^{-3} [9]).

The reduction of recombination coefficient, which had been theoretically predicted in work [7], was not tested experimentally at electron concentrations $N_e \geq 2 \times 10^{17}$ cm^{-3} . Therefore, the purpose of this work was to measure the dependence of the decay coefficient on plasma parameters experimentally and to compare it with theoretically calculated values.

Calculations for hydrogen atoms are the easiest to be carried on, because a hydrogen possesses only one electron. Discharges in water give rise to the formation of two hydrogen and one oxygen atoms (ions). At the same time, the ionization potentials for hydrogen and oxygen atoms practically coincide (they are equal to 13.595 and 13.614 eV, respectively). Therefore, the results of experimental study of the processes in such discharges are most suitable for making a comparison with the predictions made by theoretical calculations.

2. Main Part

To determine the decay coefficients, as well as the ionization and recombination ones, one has to know the concentrations of electrons (N_e) and atoms (N_a), the temperature of plasma, and the temporal dependences of those quantities. The same data are necessary for carrying out theoretical calculations [3–8].

The temperature of pulsed discharges in water and its temporal behavior were determined from the intensity of the continuous radiation emission spectrum measured at selected moments. For this purpose, the continuous or discrete in time scans of PDW radiation emission spectra were registered on high-speed “Isopanchrome” KN-4-C aerofilms (of types 24, 17, and 22*) or the films of another type. The films were calibrated by the blackening procedure, fulfilled with the help of a standard EV-45 source [10] and step attenuators [11]. Afterwards, the method of homochromatic photometry was used to determine the intensity of radiation emission by plasma and the radiance temperature at a definite wavelength and at a fixed time moment. The accuracy of the intensity determination by the method of homochromatic photometry was not worse than 10–12% [12]. Temperature measurements were executed in the spectral range 360–700 nm. The temperature was determined making use of Planck’s formula which relates the intensity of radiation emission by a blackbody to its temperature, taking the stimulated emission into account. After the reabsorbed lines having appeared, the temperature – maximal along the observation beam path

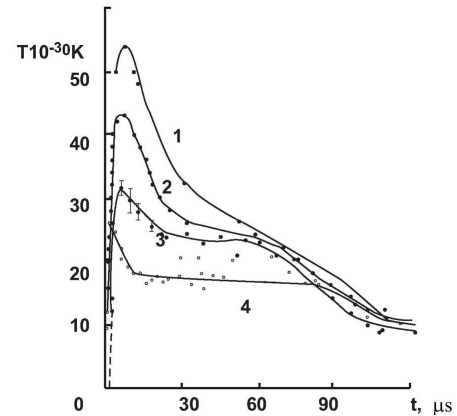


Fig. 1. Temporal dependences of the radiance temperature of PDW plasma ($W = 20$ μm , $U = 37$ kV, $l = 40$ mm, $L = 0.43$ μH) measured at various wavelengths $\lambda = 200$ (1, linear extrapolation), 400 (2), 550 (3), and 700 nm (4)

– was determined by analyzing the radiation peak intensity of the reabsorbed H_α line.

In Fig. 1, the temporal dependences of the PDW radiance temperature are depicted. One can see that the values of the radiance temperature determined at different wavelengths are substantially different; it is especially true for the initial active stage of the discharge, when an intensive input of energy into the channel occurs. As the plasma decays, the values of the radiance temperature become closer to one another. Nevertheless, in some modes, the temperatures demonstrate a two-fold difference, and the value of T_{rad} in the violet-wave range is, as a rule (at small amounts of a metal in the PDW plasma), higher than the corresponding value in the red-wave spectral range [13]. Today, there isn’t an unequivocal explanation for this deviation of the radiation emission distribution from the equilibrium one. Moreover, there is no lucidity with respect to the actual temperature in the plasma channel. At late discharge stages, when the plasma channel becomes transparent, the inverse picture can be observed, which is associated with a reduction of the channel’s optical thickness, which is different for different wavelengths. Therefore, while determining the concentration of atoms, electrons, and ions, calculations were carried out for several (two to four) values of the temperature, either measured or extrapolated into the ultra-violet region (200 nm) – the range of water transparency.

To calculate the temporal variations of pressure in the plasma channel, it is necessary to possess spatial and temporal photoscans of both the plasma channel and the



Fig. 2. Temporal photoscan of the channel radius (1) and the radius of shock-wave front (2). Illumination with a parallel light beam from a standard EV-45 source; $W = 20 \mu\text{m}$, $U = 37 \text{ kV}$, $l = 40 \text{ mm}$, and $\Delta t = 48 \mu\text{s}$

shock wave obtained with the help of illumination by an external pulsed-light source. One of the photographic records is exhibited in Fig. 2. It was used to measure the temporal variations of the channel radius r_c and the radius r_f of the shock wave front.

The data obtained for the temporal dependences of r_c and r_f were used to calculate the temporal variations of pressure in the plasma channel making use of hydrodynamic formulas; the calculations were carried out in the framework of the model of quasiincompressible liquid. This model makes allowance for the water compression between the shock-wave-front and channel radii, the temporal variations of the channel expansion rate and the shock-wave front propagation velocity, as well as the acceleration of the channel boundary. Those parameters were determined experimentally for every individual measurement; in such a way, the influence of different pressures, which were achieved in the heated vapors of metals in the course of the breakdown channel recovering after different discharges, upon the plasma parameters was excluded.

The temporal dependence of the pressure in the plasma channel was calculated by the following formulas [14]:

for cylindrical symmetry,

$$P_c = \frac{\rho_f}{2r_f} \left[2C_0 r \times \dot{r} - \dot{r}^2 r_f + 2r_f (\dot{r} r + \dot{r}^2) \ln \frac{r_f}{r} \right],$$

where $\rho_f = \rho_0 r_f^2 / (r_f^2 - r^2)$, ρ_0 is the non-perturbed liquid density, C_0 the sound velocity in the liquid, r the plasma channel radius, \dot{r} the rate of channel expansion, \dot{r}^2 the acceleration of the channel boundary, and r_f the radius of the shock-wave front;

for spherical symmetry,

$$P_c = \frac{\rho_f}{2\rho_f} \left\{ 2C_0 r^2 \dot{r} + r_f \left\{ 2r \dot{r} (r_f - r) + \right. \right.$$

$$\left. \left. + \dot{r}^2 [4(r_f - r) - r_f] \right\} \right\},$$

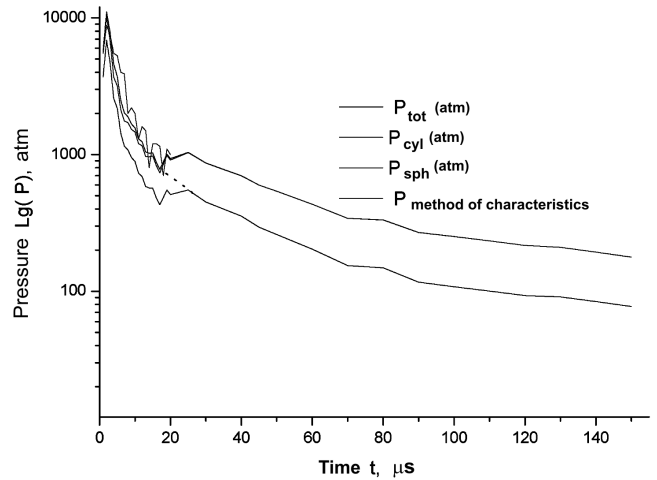


Fig. 3. Temporal dependences of the pressure in the PDW channel. $W = 20 \mu\text{m}$, $U = 37 \text{ kV}$, $l = 40 \text{ mm}$

where $\rho_f = \rho_0 r_f^3 / (r_f^3 - r^3)$. In opinion of the authors of works [14, 15], calculations by these formulas give the highest accuracy of the results obtained, provided that the rates of channel expansion are close to those measured by us experimentally. The calculation error for P_c , according to work [15], does not exceed 20%.

In Fig. 3, the typical results of calculations carried out for the temporal dependence of the pressure measured in one of the PDW modes are depicted. The calculations were executed for both symmetries – cylindrical and spherical. The latter circumstance was associated with the fact that, as was shown in work [16], when the shock wave propagates from the channel over a distance that exceeds the discharge gap width, the pressure at the front begins to fall down following the law of spherical symmetry. Another reason for changing over to the calculations of the pressure in the spherical symmetry approximation was the fact that making use of P -values obtained from the formulas corresponding to the cylindrical symmetry case gave rise to large discrepancies, when calculating the energy balance in the channel.

In this work, in order to determine the total concentration of particles, we used the equation of state for the ideal gas: $P = N^* kT$, where P is the pressure, $N^* = N_a + 2N_e$ is the total number of particles, k the Boltzmann constant, and T the temperature. According to the results of work [17], the equation of state for the ideal gas becomes transformed into

$$P = (N_a + 2N_e)kT - \frac{2}{3} e^3 \sqrt{\frac{2\pi}{kT}} N_e^{3/2} + N_a \lambda / kT, \quad (1)$$

where

$$\lambda = -\frac{\delta \ln Z_a}{\delta \ln N_e}, \quad 0 < \lambda < 1.$$

The first term on the right-hand side of Eq. (1) corresponds to the ideal gas, the second one is the Debye correction to the pressure, and the third one makes allowance for the finite number of excited bound states.

An example of the modification to the equation of state of a pure hydrogen plasma, which takes into account the formation of molecules at the increase of the atomic concentration, is presented in work [18]. The results of calculations made by the equation of state of either ideal or nonideal plasma differ by less than 20% at the parameter values $T_i = 2 \times 10^4$ K and $N_e = 10^{18}$ cm⁻³. However, this difference grows, as the temperature decreases, and can reach 100% at $T_i = 10^4$ K. As the first approximation, we neglect the probable influence of nonideality effects, because the calculation error for P is of about 20%, and the inclusion of the effects of nonideality into consideration can increase it by approximately the same magnitude. In addition to the above-described corrections, the pressure in the channel is affected by plasma compression owing to a large-amplitude current (up to 160 kA) running in it. The magnetic pressure at the peak of the current reaches about 10^8 Pa (i.e. up to 10–15% of the gas-kinetic value).

The calculations of the concentration were executed for three T_{rad} -values: two of them were measured at 400 and 700 nm, and one more was obtained by the linear extrapolation of T_{rad} into the range of 200 nm. The extrapolation was made, provided that there was no substantial jump of the radiation emission intensity in the vicinity of the Balmer series boundary ($\lambda = 360 \div 370$ nm).

The comparison of the results of T_{rad} -measurements beyond the Balmer series boundary with those obtained by extrapolating T_{rad} to the range $\lambda = 200$ nm showed that they are approximately identical. The reasons of why the calculations of the electron concentration were carried out for the limiting T_{rad} -values are that the actual plasma temperature is unknown, and the radiation emission by plasma substantially differs from that radiated by a blackbody, i.e. from the equilibrium one [13]. In work [13], the results of T_{rad} -measurements were supposed to be influenced by the temperature gradient and the atomic concentration near the channel boundary. However, the radiation that quits plasma can be affected by nonideality effects. The assumption made in work [13] cannot explain the following phenomenon in all cases: although the temperature and concentration

gradients always exist in the PDW plasma, not all studied discharge modes revealed deviations from the blackbody radiation emission distribution.

These facts and the discrepancies in the energy balance compel the choice of the temperature, at which the calculations of ionization-induced composition of plasma are to be carried out, to be made with care. For one thing, it is worthwhile to determine the limiting values of concentration, in order to evaluate the largest possible error of the N_e -calculation and, correspondingly, the decay coefficients. In this work, the Saha equation was used to calculate N_e :

$$\frac{N_e N_i}{N_a} = 4,9 \times 10^{15} \frac{G_i}{G_a} T^{3/2} \exp\left(-\frac{eE}{kT}\right). \quad (2)$$

Here, $N_{e,i,a}$ are the corresponding concentrations in cm⁻³, T is the temperature in Kelvins, G_i and G_a are the partition functions of the ground states of an ion and an atom, respectively, and E_0 is the ionization potential.

Main difficulties, which arise while finding N_e by Eq. (2), consist in calculating the partition functions and selecting the ionization potential. In opinion of the authors of works [21, 22], the ionization potential and the limiting frequency for the series boundary remain the same in nonideal plasma, as they are in an isolated atom. To calculate the partition functions, we confine ourselves to the last level observed experimentally.

The calculation of the electron concentration was carried out for hydrogen, because the ionization potentials for it and for oxygen practically do not differ from each other. Additionally, the molecules of water vapor in the channel were considered completely dissociated. We would like to point out that a full calculation of the ionization composition of water vapors at high pressures can be found in works [19, 20], where the results of calculations of the hydrogen-oxygen plasma content and electroconductivity for pressures in the range $5 \times 10^7 \div 10^9$ Pa and temperatures in the range $(10 \div 70) \times 10^3$ K were reported. The calculations were carried out in the framework of a model which takes into account quasibound states and collision complexes. However, the body of reported data is obviously insufficient for the description of a plasma channel at all stages of the PDW evolution. The plasma content was calculated in those works by applying the method of quantum-mechanical statistics for a small canonical ensemble. A comparison with the results of calculations by the Monte-Carlo method was executed, and an agreement with an

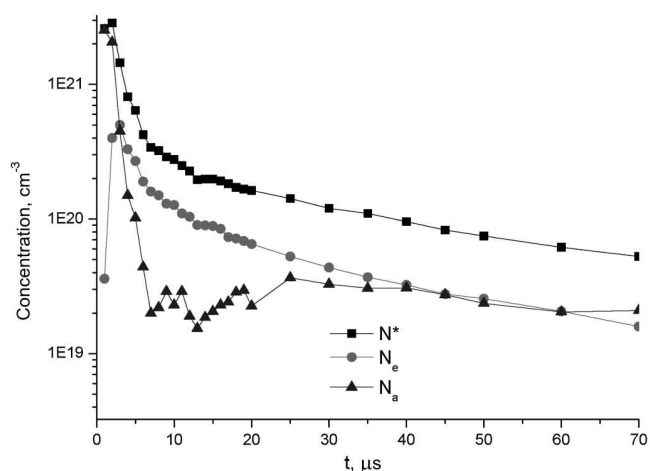


Fig. 4. Temporal dependences of the concentrations of PDW plasma components. $W = 20 \mu\text{m}$, $U = 37 \text{ kV}$, $l = 40 \text{ mm}$; T_{rad} corresponds to $\lambda = 400 \text{ nm}$

accuracy of 15% was obtained for the number-of-nuclei parameter determined by both techniques [20].

Dissociation of water molecules at all stages was not calculated in this work, because such a computation is a complicated independent task and is associated with difficulties one faces while calculating the partition functions of molecules in NP. As follows from work [20], at a pressure of $5 \times 10^8 \text{ Pa}$ and a temperature of 10^4 K , 75% of the water vapor content consists of monatomic hydrogen and oxygen; and, at a pressure of 10^8 Pa and the same temperature, their content grows up to 92%. At channel temperatures above $2 \times 10^4 \text{ K}$, water vapor can be regarded to be completely dissociated. This approximation was admitted for further calculations of the ionization composition of PDW. Therefore, the influence of H_2O , H_2 , and O_2 molecules, OH complexes, and others on the plasma content was neglected in this work.

The results of calculation of the plasma content for one of the discharge modes are presented in Fig. 4. It has to be noted that, while calculating N^* , we used the value for the brightness temperature. At the same time, if the optical thickness of plasma diminishes, then, in order that the temperature be determined, either one has to know the values of the optical thickness themselves or T_{max} has to be measured from the peak intensity of the reabsorbed hydrogen line H_α . At $\tau > 4$, the values of T_{rad} turned out underestimated and did not correspond to the actual plasma temperature; on the other hand, straightforward measurements of the optical thickness by the transmission method gave rise to overestimated values. As a result, the calculated values for N^* at the

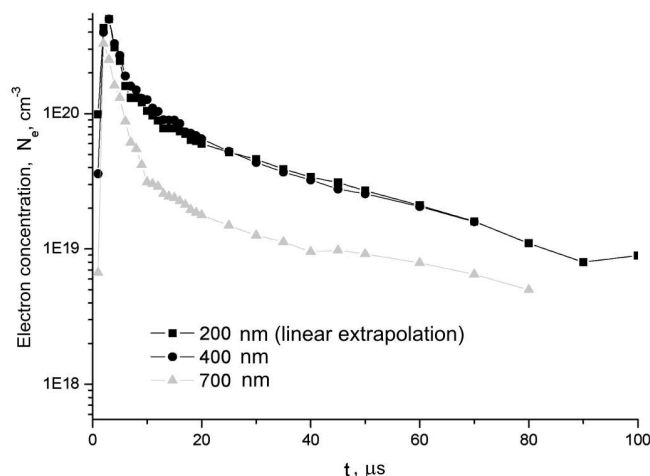


Fig. 5. Temporal dependences of the electron concentration. Calculations were carried out for the brightness temperatures obtained at different wavelengths. $W = 20 \mu\text{m}$, $U = 37 \text{ kV}$, $l = 40 \text{ mm}$

late discharge stage started to grow from a certain time moment, which contradicts the experiment, because a process of enhanced – in comparison with that at the previous time moments – recombination becomes active, as a rule, at those times.

While calculating the plasma content, we neglected the presence of metal atoms of an initiating wire in the channel (at $d = 20 \mu\text{m}$, we had $N = 2 \times 10^{17} \text{ atom/cm}^3$) and the emanation of metal vapor into plasma from the electrodes, because the amount of metal atoms was so insignificant that their presence would influence the results only if the plasma temperature decreases below $15 \times 10^3 \text{ K}$. The results of electron concentration calculations were managed to be verified experimentally only at later time moments. A reasonable accordance was achieved between the results of N_e -calculations obtained by the Saha formula and extracted from the broadening of the hydrogen line H_α in plasma microfields. The values for N_e determined by the latter technique turned out expectedly a bit larger, which evidences a certain influence of the ionization of PDW-induced metal atoms on the plasma content and a reduction of the radiation ability of nonideal plasma at $N_e > 5 \times 10^{18} \text{ cm}^{-3}$ [9].

Figure 5 demonstrates that the temporal dependences of the electron concentration calculated for the brightness temperatures determined at different wavelengths – 200 and 400 nm – are practically identical. This fact is associated with a reduction of the electron concentration owing to a decrease of the total number

of particles in a unit volume at higher temperatures and provided the same pressure. Only a lower concentration of electrons was observed, if the value of T_{rad} obtained for 700 nm was used in calculations. But the difference between N_e -values obtained did not amount to orders of magnitude.

The recombination and ionization coefficients were not managed to be determined in a straightforward manner at high temperatures (above 10^4 K) and high pressures. This circumstance stems from the joint action of two mechanisms: triple-collision recombination of electrons and atomic ionization, both being active due to a high plasma temperature. However, it allows one to determine, in practice, the coefficient of decay [2], which was done in the present work as well. Theoretical calculations of ionization and recombination were carried out separately, and the decay coefficient was determined with the help of the formula given below.

Let us calculate the experimental and theoretical coefficients of decay for the same body of data. The theoretical coefficient of decay is calculated by the formula [2,3]

$$\frac{dN_e}{dt} = N_a N_e \beta - N_e^3 \alpha, \quad (3)$$

where α is the recombination coefficient, β the ionization one, and N_e and N_a are the electron and atom concentrations, respectively. At the same time, the experimental coefficient of decay is extracted rather easily from the temporal dependence of the electron concentration. The results of calculations for dN_e/dt are exhibited in Fig. 6 (lower curve). This plot testifies that the experimental values obtained for the decay coefficient are rather small and increase with the reduction of the electron concentration. After a breakdown stimulated by the initiating wire and an intensive energy input into the PDW channel, the ionization processes prevail first; and, starting from the fifth microsecond (after the current peak having been attained), the processes of recombination become dominant. However, the decay coefficient diminishes by less than an order of magnitude (Fig. 6), if the electron concentration decreases from $5.5 \times 10^{20} \text{ cm}^{-3}$ at the 5-th microsecond to $2 \times 10^{19} \text{ cm}^{-3}$ at the 70-th one (Fig. 4) or the temperature ($\lambda = 400 \text{ nm}$) decreases from $45 \times 10^3 \text{ K}$ at the 5-th microsecond to $25 \times 10^3 \text{ K}$ at the 70-th one (Fig. 1).

While calculating the coefficient of decay theoretically, the plasma ionization and recombination coefficients were evaluated separately, and their sum was taken into consideration. In so doing, the values for

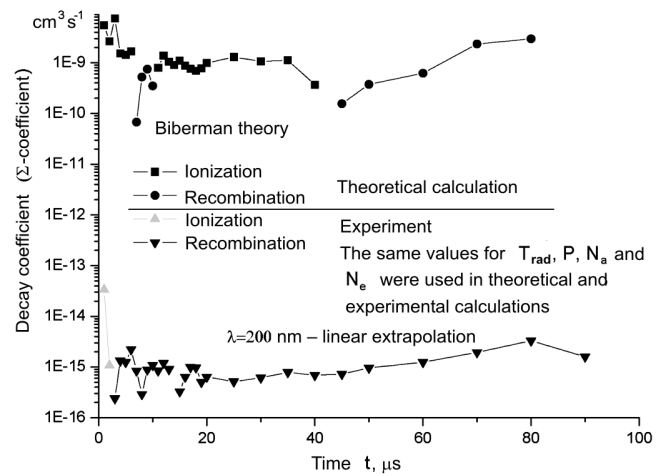


Fig. 6. Temporal dependences of the decay coefficient obtained by theoretical calculations (according to work [3]) and from our experiment

temperature and pressure (the electron concentration) were taken the same as they were at the experimental determination of the decay coefficient. The difference between the values of NP decay coefficient determined theoretically and experimentally is of about five to six orders of magnitude, with smaller values corresponding to the experimental method. This circumstance testifies to the fallaciousness of our concepts, which form the basis for calculating the coefficients of recombination and ionization in NP.

At low electron concentrations ($N_e \leq 2 \times 10^{17} \text{ cm}^{-3}$), the theoretical and experimental values of the decay coefficient (for ionization and recombination, respectively) are in rather good agreement (there is a several-fold difference between them) [2, 3]. In works [3–7], in the course of derivation of the formulas for the recombination coefficients, atoms were considered isolated, the ionization potential not to drop, and all levels of the isolated hydrogen atom were taken into account. It is characteristic that the account of recombination onto all available levels – rather than on the ground one only – of the hydrogen atom gives rise to a 2 to 3-fold increase of the recombination coefficient at temperatures of $(4 \div 62) \times 10^3 \text{ K}$ [4]. If the electron concentration grows above $N_e \approx 10^{18} \text{ cm}^{-3}$, the intrinsic plasma microfields start to substantially affect the ionization potential, the level broadening (owing to the Stark effect), the “exclusion” of upper levels (the line $H_\alpha = 656.2 \text{ nm}$ included), and so on.

In work [5], the coefficient of electron recombination was demonstrated to increase, if the recombination

onto upper levels is made allowance for. Moreover, this increase can be two orders of magnitude larger than the radiation recombination. However, the corresponding calculations were carried out for electron concentrations of $10^{12} - 10^{13} \text{ cm}^{-3}$. At the same time, in NP, upper levels become “excluded” [21], i.e. disappear, under the action of plasma microfields. This effect can explain, to some extent, the disagreement between theoretical and experimental values obtained for the coefficient of NP decay, but cannot explain such large discrepancies which were obtained in this work.

In work [8], a first attempt was made to consider the influence of plasma nonideality on the recombination coefficient for dense plasma. However, according to the results of work [8], the ratios between the recombination coefficient values amount to about 4.5 and 1.5 at the electron concentration of 10^{20} cm^{-3} and the temperatures of $(8 \div 16) \times 10^3 \text{ K}$, respectively. It should be pointed out that the coefficients of capture onto realized levels were assumed in this work to be close to the value of $\alpha_n N_e$ calculated for an isolated atom. No calculations are available for higher plasma temperatures, but it is clear that the discrepancy between the recombination coefficients would be even smaller. It is worth noting that, in this work, we did not take into account the large broadening of lower realized levels, which can be equal to several tens of nanometers [9]. We also neglected the reduction of the electric field potential of a hydrogen nucleus in plasma microfields, although these microfields are strong enough, being comparable with the fields of the nucleus itself. This effect can also influence rather strongly the magnitude of recombination (decay) coefficient.

It should be noted that the decay coefficient increases and approaches the values determined theoretically, as the electron concentration diminishes. The theoretical results and experimental data which were obtained for one mode of the discharges, in which the electron concentration N_e and the temperature were managed to be measured up to $2 \times 10^{17} \text{ cm}^{-3}$ and $8 \times 10^3 \text{ K}$, respectively, revealed an approximately the same agreement as was obtained in work [2].

3. Conclusions

The decay coefficients for NP with the concentration of electrons from 5×10^{20} to 10^{19} cm^{-3} and in the temperature interval $(20 \div 45) \times 10^3 \text{ K}$ have been measured experimentally and calculated theoretically. The experimental data turned out larger by 5–6 orders of magnitude. Any theoretical explanation for such a large

discrepancy is absent. As the electron concentration and the temperature decrease, the gap between experimental and calculated values of the plasma decay coefficient becomes narrower. The theoretical calculations were based on the model of interaction between an electron and an isolated atom; they did not take into consideration the reduction of the ionization potentials, the disappearance of the majority of levels in plasma microfields, and the strong broadening of realized atomic levels. For the relevant theory to be constructed correctly, all those factors must be taken into account.

1. V.E. Fortov and I.T. Yakubov, *Physics of Nonideal Plasma* (Hemisphere, New York, 1989).
2. O.A. Malkin, *Pulse Current and Relaxation in Gas* (Atomizdat, Moscow, 1974) (in Russian).
3. L.M. Biberman, V.S. Vorob'ev, and I.T. Yakubov, *Kinetics of Nonequilibrium Low-Temperature Plasmas* (Consultants Bureau, New York, 1987).
4. D.R. Bates and A. Dalgarno, in *Atomic and Molecular Processes*, edited by D.R. Bates (Academic Press Inc., New York, 1962), p. 249.
5. D'Angelo, *Phys. Rev.* **121**, 505 (1961).
6. L.M. Biberman, V.S. Vorob'ev, and I.T. Yakubov, *Usp. Fiz. Nauk* **107**, 353.
7. L. Popova, G. Kamberov, T. Nickolov, et al., *Bulg. J. Phys.* **32**, 263 (2005).
8. Yu.K. Kurilenkov, *Teplotiz. Vysok. Temp.* **18**, 1312 (1980).
9. V.V. Matvienko, A.Yu. Popov, and O.A. Fedorovich, in *Theory, Experiment, and Practice of Pulsed-Discharge Technology* (Naukova Dumka, Kyiv, 1987), p. 14 (in Russian).
10. A.N. Demidov, N.N. Ogurtsova, and I.V. Podmoshensky, *Optiko-Mekhan. Promyshl. N 1, 2* (1960).
11. L.L. Pasechnik, P.D. Starchik, and O.A. Fedorovich, in *Theory, Experiment, and Practice of Pulsed-Discharge Technology* (Naukova Dumka, Kyiv, 1987) (in Russian), p. 6.
12. V.I. Malyshev, *Introduction to Experimental Spectroscopy* (Nauka, Moscow, 1979) (in Russian).
13. L.L. Pasechnik, P.D. Starchik, and O.A. Fedorovich, in *Abstracts of the 6-th All-Union Conference on Physicist of Low-Temperature Plasma* (Leningrad, 1983), Vol. 1, p. 501 (in Russian).
14. N.M. Beskaravainyi and V.A. Pozdeev, in *Physical and Mechanical Processes at High-Voltage Discharge in Liquid* (Naukova Dumka, Kyiv, 1980), p. 88 (in Russian).
15. N.M. Beskaravainyi and V.A. Pozdeev, Report on the Project N 149/20 (Nikolaev, 1980) (in Russian).
16. Y.F. Hamman, *Z. Angew. Phys. B* **31**, S133 (1971).
17. L.P. Kudrin, *Statistical Plasma Physics* (Atomizdat, Moscow, 1974) (in Russian).

18. K.A. Naugolnykh and N.A. Roi, *Electrical Discharges in Water* (Nauka, Moscow, 1971) (in Russian).
19. V.V. Ivanov, I.S. Shvets, and A.V. Ivanov, *Underwater Spark Discharges* (Naukova Dumka, Kyiv, 1982) (in Russian).
20. P.I. Tsarenko, A.R. Rizun, M.V. Zhirnov, and V.V. Ivanov, *Hydrodynamics and Thermal Characteristics of Powerful Underwater Spark Discharges* (Naukova Dumka, Kyiv, 1984) (in Russian).
21. G.A. Kobzev, Yu.K. Kurilenkov, and G.E. Norman, *Teplofiz. Vysok. Temp.* **15**, 193 (1977).
22. G.E. Norman, *Teplofiz. Vysok. Temp.* **17**, 453 (1979).

Translated from Ukrainian by O.I. Voitenko

ЕКСПЕРИМЕНТАЛЬНІ ДОСЛІДЖЕННЯ КОЕФІЦІЄНТА РОЗПАДУ НЕІДЕАЛЬНОЇ ПЛАЗМИ ІМПУЛЬСНИХ РОЗРЯДІВ У ВОДІ

О.А. Федорович, Л.М. Войтенко

Р е з ю м е

Наведено результати експериментального визначення коефіцієнта розпаду неідеальної плазми (НП) імпульсного розряду у воді (ІРВ) для одного з режимів розряду. Порівняно результати експерименту з теоретичними розрахунками. Виявлено розбіжність між експериментальними і розрахованими значеннями коефіцієнтів розпаду, яка становить 5–6 порядків. Менші значення одержано для експериментальних коефіцієнтів розпаду. Існуючі теоретичні моделі не можуть забезпечити задовільного узгодження з експериментом, отже потрібна подальша розробка моделі рекомбінації НП.